Critical hopping parameter in $O(a)$ improved lattice QCD

H. Panagopoulos* and Y. Proestos†
Department of Physics, University of Cyprus, P.O. Box 20537, Nicosia CY-1678, Cyprus
(Received 16 August 2001; published 12 December 2001)

We calculate the critical value of the hopping parameter, κ_c, in $O(a)$ improved lattice QCD, to two loops in perturbation theory. We employ the Sheikholeslami-Wohlert (clover) improved action for Wilson fermions. The quantity which we study is a typical case of a vacuum expectation value resulting in an additive renormalization; as such, it is characterized by a power (linear) divergence in the lattice spacing, and its calculation lies at the limits of applicability of perturbation theory. The dependence of our results on the number of colors N, the number of fermionic flavors, N_f, and the clover parameter $c_{\rm SW}$ is shown explicitly. We compare our results with nonperturbative evaluations of κ_c coming from Monte Carlo simulations.

DOI: 10.1103/PhysRevD.65.014511 PACS number(s): 11.15.Ha, 12.38.Gc

I. INTRODUCTION

In this paper we calculate the critical value of the hopping parameter κ_c in lattice QCD, to two loops in perturbation theory. We employ the $O(a)$ improved Sheikholeslami-Wohlert [1] (clover) action for Wilson fermions; this action is widely used now in Monte Carlo simulations as a means of reducing finite lattice spacing effects, leading to a faster approach to the continuum.

The Wilson fermionic action is a standard implementation of fermions on the lattice. It circumvents the notorious doubling problem by means of a higher derivative term, which removes unphysical propagator poles and has a vanishing classical continuum limit; at the same time, the action is strictly local, which is very advantageous for numerical simulation. The price one pays for strict locality and absence of doublers is, of course, well known: The higher derivative term breaks chiral invariance explicitly. Thus, merely setting the bare fermionic mass to zero is not sufficient to ensure chiral symmetry in the quantum continuum limit; quantum corrections introduce an additive renormalization to the fermionic mass, which must then be fine-tuned to have a vanishing renormalized value. Consequently, the hopping parameter κ, which is very simply related to the fermion mass, must be appropriately shifted from its naive value, in order to recover chiral invariance.

By dimensional power counting, the additive mass renormalization is seen to be linearly divergent with the lattice spacing. This adverse feature of Wilson fermions, typical of vacuum expectation values of local objects, poses an additional problem to a perturbative treatment, aside from the usual issues related to lack of Borel summability. Indeed, our calculation serves as a check on the limits of applicability of perturbation theory, by comparison with non perturbative results coming from Monte Carlo simulations.

In the present work we will follow the procedure and notation of Ref. [2], in which κ_c was computed using the Wilson fermionic action without $O(a)$ improvement. The results of Ref. [2] were recently confirmed in Ref. [3], in which a coordinate space method was used to achieve even greater accuracy.

The critical fermionic mass and hopping parameter will now depend not only on the number of colors N and of fermionic flavors N_f, but also on the free parameter $c_{\rm SW}$ which appears in the clover action (see next section); we will keep this dependence explicit in our results.

In Sec. II we define the quantities which we set out to compute, and describe our calculation. In Sec. III we present our results and compare with Monte Carlo evaluations. Finally, in Sec. IV we obtain improved estimates coming from a tadpole resummation.

II. FORMULATION OF THE PROBLEM

Our starting point is the Wilson formulation of the QCD action on the lattice, with the addition of the clover (SW) [1] fermion term. Its action reads, in standard notation,

$$\begin{aligned} S_L=&\frac{1}{g_0^2}\sum_{x,\mu,\nu}\mathrm{Tr}[1-U_{\mu,\nu}(x)] \\ &+\sum_f\sum_x(4r+m_B)\bar{\psi}_f(x)\psi_f(x) \\ &-\frac{1}{2}\sum_f\sum_{x,\mu}[\bar{\psi}_f(x)(r-\gamma_\mu)U_\mu(x)\psi_f(x+\hat{\mu}) \\ &\qquad+\bar{\psi}_f(x+\hat{\mu})(r+\gamma_\mu)U_\mu(x)^\dagger\psi_f(x)] \\ &+\frac{i}{4}c_{\rm SW}\sum_f\sum_{x,\mu,\nu}\bar{\psi}_f(x)\sigma_{\mu\nu}\hat{F}_{\mu\nu}(x)\psi_f(x), \end{aligned} \tag{1}$$

where

$$\hat{F}_{\mu\nu}\equiv\frac{1}{8}(Q_{\mu\nu}-Q_{\nu\mu}),$$

$$Q_{\mu\nu}=U_{\mu,\nu}+U_{\nu,-\mu}+U_{-\mu,-\nu}+U_{-\nu,\mu}. \tag{2}$$

Here $U_{\mu,\nu}(x)$ is the usual product of link variables $U_\mu(x)$ along the perimeter of a plaquette in the μ-ν directions,

*Email address: haris@ucy.ac.cy
†Present address: Department of Physics, Ohio State University, Columbus, OH 43210. Email address: yiannis@mps.ohio-state.edu

originating at x; g_0 denotes the bare coupling constant; r is the Wilson parameter; f is a flavor index; $\sigma_{\mu\nu}=(i/2)[\gamma_\mu,\gamma_\nu]$. Powers of the lattice spacing a have been omitted and may be directly reinserted by dimensional counting.

We use the standard covariant gauge-fixing term; in terms of the vector field $Q_\mu(x)(U_\mu(x)=\exp[ig_0Q_\mu(x)])$, it reads

$$S_{gf}=\lambda_0\sum_{\mu,\nu}\sum_x \mathrm{Tr}\,\Delta^-_\mu Q_\mu(x)\Delta^-_\nu Q_\nu(x),$$

$$\Delta^-_\mu Q_\nu(x)\equiv Q_\nu(x-\hat{\mu})-Q_\nu(x). \tag{3}$$

Having to compute a gauge invariant quantity, we chose to work in the Feynman gauge, $\lambda_0=1$. Covariant gauge fixing produces the following action for the ghost fields ω and $\bar{\omega}$:

$$\begin{aligned}S_{gh}=2\sum_x\sum_\mu \mathrm{Tr}[\Delta^+_\mu\omega(x)]^\dagger\{&\Delta^+_\mu\omega(x)\\&+ig_0[Q_\mu(x),\omega(x)]+\tfrac{1}{2}ig_0[Q_\mu(x),\Delta^+_\mu\omega(x)]\\&-\tfrac{1}{12}g_0^2[Q_\mu(x),[Q_\mu(x),\Delta^+_\mu\omega(x)]]+\cdots\},\end{aligned}$$

$$\Delta^+_\mu\omega(x)\equiv\omega(x+\hat{\mu})-\omega(x). \tag{4}$$

Finally the change of integration variables from links to vector fields yields a Jacobian that can be rewritten as the usual measure term S_m in the action:

$$S_m=\frac{1}{12}Ng_0^2\sum_x\sum_\mu \mathrm{Tr}\,Q_\mu(x)Q_\mu(x)+\cdots. \tag{5}$$

In S_{gh} and S_m we have written out only terms relevant to our computation. The full action is: $S=S_L+S_{gf}+S_{gh}+S_m$.

The bare fermionic mass m_B must be set to zero for chiral invariance in the classical continuum limit. The value of the parameter c_{SW} can be chosen arbitrarily; it is normally tuned in a way as to minimize $O(a)$ effects. Terms proportional to r in the action, as well as the clover terms, break chiral invariance. They vanish in the classical continuum limit; at the quantum level, they induce nonvanishing, flavor-independent corrections to the fermion masses. Numerical simulation algorithms usually employ the hopping parameter,

$$\kappa\equiv\frac{1}{2m_Ba+8r} \tag{6}$$

as an adjustable quantity. Its critical value, at which chiral symmetry is restored, is thus $1/8r$ classically, but gets shifted by quantum effects.

The renormalized mass can be calculated in textbook fashion from the fermion self-energy. Denoting by $\Sigma^L(p,m_B,g_0)$ the truncated, one particle irreducible fermionic two-point function, we have for the fermionic propagator:

$$S(p)=[i\mathring{p}+m(p)-\Sigma^L(p,m_B,g_0)]^{-1} \tag{7}$$

where

$$\mathring{p}=\sum_\mu \gamma_\mu\frac{1}{a}\sin(ap^\mu),\quad m(p)=m_B+\frac{2r}{a}\sum_\mu \sin^2(ap^\mu/2).$$

To restore the explicit breaking of chiral invariance, we require that the renormalized mass vanish:

$$S^{-1}(0)=0\Rightarrow m_B=\Sigma^L(0,m_B,g_0). \tag{8}$$

The above is a recursive equation for m_B, which can be solved order by order in perturbation theory.

We write the loop expansion of Σ^L as:

$$\Sigma^L(0,m_B,g_0)=g_0^2\Sigma^{(1)}+g_0^4\Sigma^{(2)}+\cdots. \tag{9}$$

Two diagrams contribute to $\Sigma^{(1)}$, shown in Fig. 1. In these diagrams, the fermion mass must be set to its tree level value, $m_B\to 0$.

The quantity $\Sigma^{(2)}$ receives contributions from a total of 26 diagrams, shown in Fig. 2. Genuine 2-loop diagrams must again be evaluated at $m_B\to 0$; in addition, one must include to this order the 1-loop diagram containing an $O(g_0^2)$ mass counterterm (diagram 23).

The contribution of the i^{th} diagram can be written in the form

$$(N^2-1)\cdot\sum_{j=0}^{4}\left(c^{(j)}_{1,i}+\frac{c^{(j)}_{2,i}}{N^2}+\frac{N_f}{N}c^{(j)}_{3,i}\right)c_{\mathrm{SW}}{}^j, \tag{10}$$

where $c^{(j)}_{1,i},c^{(j)}_{2,i},c^{(j)}_{3,i}$ are numerical constants. The dependence on c_{SW} is seen to be polynomial of degree 4, as can be verified by inspection of Fig. 2.

Certain sets of diagrams, corresponding to renormalization of loop propagators, must be evaluated together in order to obtain an infrared-convergent result: These are diagrams 7+8+9+10+11, 12+13, 14+15+16+17+18, 19+20, 21+22+23.

III. NUMERICAL RESULTS

Evaluating the two diagrams of Fig. 1, we find for $\Sigma^{(1)}$:

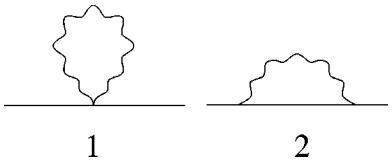

FIG. 1. One-loop diagrams contributing to Σ^L. Wavy (solid) lines represent gluons (fermions).

$$\Sigma^{(1)}=\frac{N^2-1}{N}[-0.154\,933\,390\,231\,060\,21 \quad \text{(diagram 1)}$$
$$-0.007\,923\,668\,479\,79(1)+c_{\rm SW}\ 0.043\,483\,033\,882\,05(10)$$
$$+c_{\rm SW}{}^2\ 0.018\,095\,768\,781\,42(1)] \quad \text{(diagram 2)}. \tag{11}$$

Here and below we set r to its usual value, $r=1$. One- and two-loop results pertaining to $c_{\rm SW}=0$ are as in Ref. [2], and can be found with greater accuracy in Ref. [3].

For $c_{\rm SW}\neq 0$, only one-loop results exist so far in the literature; a recent presentation for the case $c_{\rm SW}=1$ (see Ref. [4] and earlier references therein) is in perfect agreement with our Eq. (11):

$$\Sigma^{(1)}(N=3,c_{\rm SW}=1)=-0.270\,075\,349\,5(2) \quad \text{(Ref. [4])}$$
$$-0.270\,075\,349\,459\,7(5) \quad \text{[the present work, Eq. (11)]}. \tag{12}$$

It should be clear to the reader that such a high level of precision is hardly relevant *per se*, especially given the expected deviation from nonperturbative results; nevertheless, it serves as a testing ground for both accuracy and efficiency of our methods, in view of the more demanding higher loop calculations. Further, high precision is called for in the context of the Schrödinger functional computation, to permit a stable extrapolation of various parameters to infinite lattice (see Ref. [4]). Regarding efficiency, let us note that the numerical integrations leading to Eq. (11) require a mere $\sim$10 min of CPU time on a typical 1 GHz Pentium III processor.

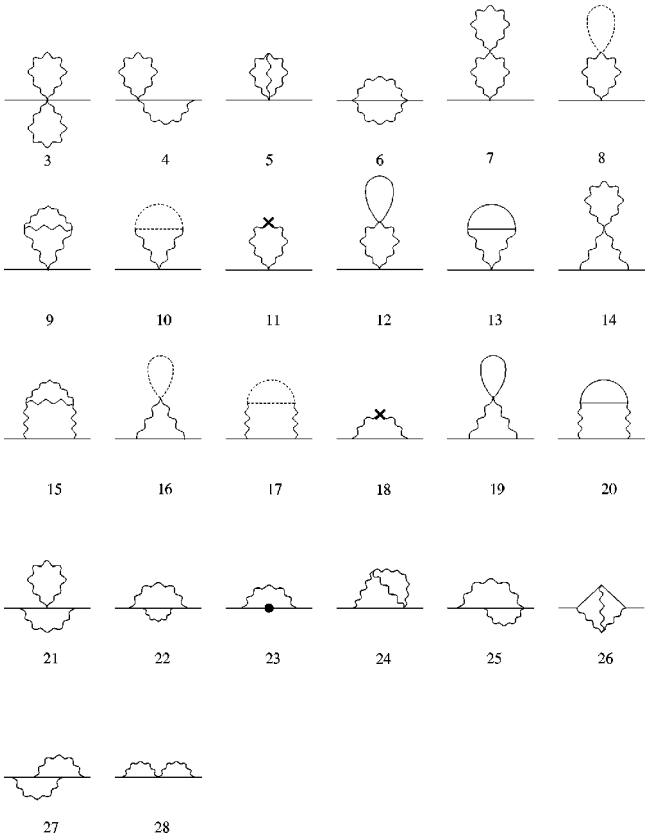

FIG. 2. Two-loop diagrams contributing to Σ^L. Wavy (solid, dotted) lines represent gluons (fermions, ghosts). Crosses denote vertices stemming from the measure part of the action; a solid circle is a fermion mass counterterm.

We now turn to the much more cumbersome evaluation of the two-loop diagrams, which is the crux of our present computation. As in Ref. [2], we use a MATHEMATICA package which we have developed for symbolic manipulations in lattice perturbation theory (see, e.g., Ref. [5]). For the purposes of the present work (and a related work on the β-function [6]), we have augmented the package to include the vertices of the clover action.

In Tables I, II, III, and IV we present the values of the coefficients $c^{(1)}_{k,i}$, $c^{(2)}_{k,i}$, $c^{(3)}_{k,i}$, $c^{(4)}_{k,i}$, respectively. The $O(c_{\rm SW}{}^0)$ coefficients $c^{(0)}_{k,i}$ are as in Ref. [2], and have been listed in Table V for completeness. Diagrams giving vanishing contributions to a given power of $c_{\rm SW}$ have been omitted from the corresponding table.

The momentum integrations leading to the values of each coefficient are performed numerically on lattices of varying size $L\leqslant 32$, and then extrapolated to infinite lattice size using a broad spectrum of functional forms of the type $\Sigma_{i,j}e_{ij}(\ln L)^j/L^i$. The systematic error resulting from the extrapolations has been estimated rather conservatively using the procedure of Ref. [5], and has been included in the tables.

One important consistency check can be performed on those diagrams which are separately IR divergent; taken together in groups, as listed at the end of Sec. II, they give finite and very stable extrapolations for the coefficients of each power of $c_{\rm SW}$. Several other consistency checks stem from exact relations among various coefficients; to name a few:

$$c^{(1)}_{2,4}=b^{(1)}_2(1/2-b^{(0)}_1)/4,$$
$$c^{(2)}_{2,4}=b^{(2)}_2/4,$$
$$c^{(0)}_{2,7}=-b^{(0)}_1 3/32, \tag{13}$$
$$c^{(1)}_{2,14}=-b^{(1)}_2/8,$$
$$c^{(2)}_{2,14}=-b^{(2)}_2/8.$$

TABLE I. Coefficients $c_{1,i}^{(1)}$, $c_{2,i}^{(1)}$, $c_{3,i}^{(1)}$. $r=1$.

i	$c_{1,i}^{(1)}$	$c_{2,i}^{(1)}$	$c_{3,i}^{(1)}$
4	−0.006 972 989 69(1)	0.007 119 622 70(1)	0
12+13	0	0	−0.000 055 40(1)
14+15+16+17+18	0.005 587(1)	−0.005 435 6(3)	0
19+20	0	0	−0.000 490 5(2)
21+22+23	0.001 549 9(6)	−0.001 549 9(6)	0
24	−0.000 227 42(6)	0	0
25	0.001 471 5(3)	−0.000 027 52(1)	0
26	0.000 943 9(2)	0	0
27	0	−0.000 752 5(1)	0
28	0.000 248 87(3)	0.000 086 138(5)	0

Here, $b_i^{(j)}$ are the coefficients of the ith 1-loop diagram, multiplying $c_{\rm SW}{}^j$, as displayed in Eq. (11). Comparing with our numerical values of Tables I–IV, we find agreement well within the error bars.

Leaving the choice of values for N, N_f, and $c_{\rm SW}$ unspecified, our result takes the form:

$$\begin{aligned}\Sigma^{(2)}=(N^2-1)\{&[-0.017\,537(3) &&+1/N^2\ 0.016\,567(2) &&+N_f/N\ 0.001\,186\,18(8)]\\ &+[0.002\,601(2) &&-1/N^2\ 0.000\,559\,7(7) &&-N_f/N\ 0.000\,545\,9(2)]\ c_{\rm SW}\\ &+[-0.000\,155\,6(3) &&+1/N^2\ 0.002\,622\,6(2) &&+N_f/N\ 0.001\,365\,2(1)]\ c_{\rm SW}{}^2\\ &+[-0.000\,163\,15(6) &&+1/N^2\ 0.000\,158\,03(6) &&-N_f/N\ 0.000\,692\,25(3)]\ c_{\rm SW}{}^3\\ &+[-0.000\,017\,219(2) &&+1/N^2\ 0.000\,042\,829(3) &&-N_f/N\ 0.000\,198\,100(7)]\ c_{\rm SW}{}^4\}. \end{aligned} \tag{14}$$

To make more direct contact with non-perturbative results, we evaluate $\Sigma^{(2)}$ at $N=3$ and $N_f=0,2$, obtaining:

$$\begin{aligned}\Sigma^{(2)}(N=3,N_f=0)=\ &-0.125\,57(3)+0.020\,31(2)\ c_{\rm SW}+0.001\,087(3)\ c_{\rm SW}{}^2\\ &-0.001\,165(1)\ c_{\rm SW}{}^3-0.000\,099\,68(2)\ c_{\rm SW}{}^4,\end{aligned}$$

$$\begin{aligned}\Sigma^{(2)}(N=3,N_f=2)=\ &-0.119\,24(3)+0.017\,40(2)\ c_{\rm SW}+0.008\,368(3)\ c_{\rm SW}{}^2\\ &-0.004\,857(1)\ c_{\rm SW}{}^3-0.001\,156\,2(1)\ c_{\rm SW}{}^4.\end{aligned} \tag{15}$$

TABLE II. Coefficients $c_{1,i}^{(2)}$, $c_{2,i}^{(2)}$, $c_{3,i}^{(2)}$. $r=1$.

i	$c_{1,i}^{(2)}$	$c_{2,i}^{(2)}$	$c_{3,i}^{(2)}$
4	−0.004 869 170 62(1)	0.004 523 942 20(1)	0
6	0.001 753 8(2)	0	0
12+13	0	0	0.000 894 9(1)
14+15+16+17+18	0.002 197 7(2)	−0.002 262 0(2)	0
19+20	0	0	0.000 470 3(1)
21+22+23	−0.000 186 4(1)	0.000 186 4(1)	0
24	0.000 032 57(1)	0	0
25	−0.000 228 29(1)	−0.000 059 15(1)	0
26	0.000 608 75(1)	0	0
27	0	0.000 351 68(2)	0
28	0.000 535 39(5)	−0.000 118 18(1)	0

TABLE III. Coefficients $c_{1,i}^{(3)}$, $c_{2,i}^{(3)}$, $c_{3,i}^{(3)}$. $r=1$.

i	$c_{1,i}^{(3)}$	$c_{2,i}^{(3)}$	$c_{3,i}^{(3)}$
19+20	0	0	−0.000 692 25(3)
21+22+23	−0.000 175 30(6)	0.000 175 30(6)	0
25	0.000 022 090(4)	0	0
26	−0.000 023 954(3)	0	0
27	0	−0.000 017 264(2)	0
28	0.000 014 014(3)	0	0

Equations (11), (15) lead immediately to the 1- and 2-loop results for the critical mass: $m_c^{(1)}=g_0^2\Sigma^{(1)}$, $m_c^{(2)}=g_0^2\Sigma^{(1)}+g_0^4\Sigma^{(2)}$, and the corresponding hopping parameter $\kappa_c=1/(2m_ca+8r)$.

A number of non-perturbative determinations of κ_c exist in the literature for particular values of $\beta=2N/g_0^2$ and $c_{\rm SW}=0$, see e.g., Refs. [7,8] (quenched case) and Refs. [9,10] (unquenched, $N_f=2$). We present these in Table VI, together with the 1- and 2-loop results ($\kappa_c^{(1)}$, $\kappa_c^{(2)}$). Also included in the table are the improved results obtained with the method described in the following section.

IV. IMPROVED PERTURBATION THEORY

In order to obtain improved estimates from lattice perturbation theory, one may perform a resummation to all orders of the so-called ''cactus'' diagrams [11–13]. Briefly stated, these are gauge-invariant tadpole diagrams which become disconnected if any one of their vertices is removed. The original motivation of this procedure is the well known observation of ''tadpole dominance'' in lattice perturbation theory. In the following we adapt the calculation of Ref. [2] to the clover action. We refer to Ref. [11] for definitions and analytical results.

Since the contribution of standard tadpole diagrams is not gauge invariant, the class of gauge invariant diagrams we are considering needs further specification. By the Baker-Campbell-Hausdorff (BCH) formula, the product of link variables along the perimeter of a plaquette can be written as

TABLE IV. Coefficients $c_{1,i}^{(4)}$, $c_{2,i}^{(4)}$, $c_{3,i}^{(4)}$. $r=1$.

i	$c_{1,i}^{(4)}$	$c_{2,i}^{(4)}$	$c_{3,i}^{(4)}$
19+20	0	0	−0.000 198 10(1)
21+22+23	−0.000 017 219(2)	0.000 017 219(2)	0
27	0	0.000 025 610(2)	0

$$\begin{aligned} U_{x,\mu\nu} &= e^{ig_0A_{x,\mu}}e^{ig_0A_{x+\mu,\nu}}e^{-ig_0A_{x+\nu,\mu}}e^{-ig_0A_{x,\nu}} \\ &= \exp\{ig_0(A_{x,\mu}+A_{x+\mu,\nu}-A_{x+\nu,\mu}-A_{x,\nu})+O(g_0^2)\} \\ &= \exp\{ig_0F_{x,\mu\nu}^{(1)}+ig_0^2F_{x,\mu\nu}^{(2)}+O(g_0^4)\}. \end{aligned} \tag{16}$$

The diagrams that we propose to resum to all orders are the cactus diagrams made of vertices containing $F_{x,\mu\nu}^{(1)}$. Terms of this type come from the pure gluon part of the lattice action. These diagrams dress the transverse gluon propagator P_A leading to an improved propagator $P_A^{(I)}$, which is a multiple of the bare transverse one:

$$P_A^{(I)}=\frac{P_A}{1-w(g_0)}, \tag{17}$$

where the factor $w(g_0)$ will depend on g_0 and N, but not on the momentum. The function $w(g_0)$ can be extracted by an appropriate algebraic equation that has been derived in Ref. [11] and that can be easily solved numerically; for $SU(3)$, $w(g_0)$ satisfies

$$ue^{-u/3}[u^2/3-4u+8]=2g_0^2, \quad u(g_0)\equiv\frac{g_0^2}{4[1-w(g_0)]}. \tag{18}$$

The vertices coming from the gluon part of the action, Eq. (1), get also dressed using a procedure similar to the one leading to Eq. (17) [11]. Vertices coming from the Wilson part of the fermionic action stay unchanged, since their definition contains no plaquettes on which to apply the linear

TABLE V. Coefficients $c_{1,i}^{(0)}$, $c_{2,i}^{(0)}$, $c_{3,i}^{(0)}$. $r=1$.

i	$c_{1,i}^{(0)}$	$c_{2,i}^{(0)}$	$c_{3,i}^{(0)}$
3	0.002 000 362 950 707 492	−0.003 000 544 426 061 237 5	0
4	0.000 409 213 61(1)	−0.000 613 820 41(2)	0
6	−0.000 048 889 1(8)	0.000 097 778(2)	0
7+8+9+10+11	−0.013 927(3)	0.014 525(2)	0
12+13	0	0	0.000 792 63(8)
14+15+16+17+18	−0.005 753(1)	0.005 832 3(7)	0
19+20	0	0	0.000 393 556(7)
21+22+23	0.000 096 768(4)	−0.000 096 768(4)	0
25	0.000 077 62(1)	−0.000 155 24(3)	0
26	−0.000 400 00(5)	0	0
27	0	−0.000 006 522(1)	0
28	0.000 007 848 2(5)	−0.000 015 696(1)	0

TABLE VI. One- and two-loop results ($\kappa_c^{(1)}$, $\kappa_c^{(2)}$), along with their improved (dressed) counterparts, and nonperturbative determinations. See references, shown in square brackets, for details on the nonperturbative definition of κ and on error estimates.

N_f	β	$c_{\rm SW}$	$\kappa_c^{(1)}$	$\kappa_c^{(2)}$	$\kappa_{c,\,\rm dressed}^{(1)}$	$\kappa_{c,\,\rm dressed}^{(2)}$	Simulation	
0	5.70	1.568	0.1296	0.1332	0.1366	0.1366	0.1432	[8]
0	6.00	1.479	0.1301	0.1335	0.1362	0.1362	0.1392	[8]
0	6.00	1.769	0.127 49	0.130 61	0.133 72	0.133 19	0.135 25	[8,7]
0	6.20	1.442	0.1303	0.1334	0.1358	0.1358	0.1379	[8]
0	6.20	1.614	0.128 78	0.131 82	0.134 39	0.134 14	0.135 82	[8,7]
0	12.0	1.1637	0.128 766	0.129 622	0.129 807	0.129 845	0.129 909	[7]
0	24.0	1.0730	0.127 019	0.127 229	0.127 243	0.127 253	0.127 258	[7]
2	5.20	2.0171	0.12515	0.129 87	0.134 81	0.133 42	0.136 63	[10,9]
2	2.26	1.9497	0.125 89	0.130 43	0.135 17	0.133 92	0.137 09	[10,9]
2	2.29	1.9192	0.126 22	0.130 68	0.135 32	0.134 14	0.137 30	[10,9]

BCH formula; the 3- and 4-point vertices of the clover action, on the other hand, acquire simply a factor of $[1-w(g_0)]$ [12].

One can apply the resummation of cactus diagrams to the calculation of additive and multiplicative renormalizations of lattice operators. Applied to a number of cases of interest [11,12], this procedure yields remarkable improvements when compared with the available nonperturbative estimates. As regards numerical comparison with other improvement schemes (tadpole improvement, boosted perturbation theory, etc.) [14,15], cactus resummation fares equally well on all the cases studied [13].

One advantageous feature of cactus resummation, in comparison to other schemes of improved perturbation theory, is the possibility of systematically incorporating higher loop diagrams. The present calculation exemplifies this feature, as we will now show.

Dressing the 1-loop results is quite straightforward: the fermionic propagator stays unchanged, the gluon propagator gets multiplied by $1/[1-w(g_0)]$ and the dressing of the fermionic vertices amounts to a rescaling: $c_{\rm SW}\to c_{\rm SW}[1-w(g_0)]$. The resulting values, $\kappa_{c,\,\rm dressed}^{(1)}$, are shown in Table VI. It is worth noting that these values already fare better than the much more laborious undressed 2-loop results.

We now turn to dressing the 2-loop results. Here, one must take care to avoid double counting: A part of diagrams 4, 7 and 14 has already been included in dressing the 1-loop result, and must be explicitly subtracted from $\Sigma^{(2)}$ before dressing. Fortunately, this part (we shall denote it by $\Sigma_{\rm sub}^{(2)}$) is easy to identify, as it necessarily includes all of the $1/N^2$ part in diagrams 7, 14, and the $1/N^2$ part of diagram 4 involving a clover 5-point vertex. A simple exercise in contraction of $SU(N)$ generators shows that $\Sigma_{\rm sub}^{(2)}$ is proportional to $(2N^2-3)(N^2-1)/(3N^2)$. There follows without difficulty that:

$$\Sigma_{\rm sub}^{(2)}=-(2N^2-3)(N^2-1)/(3N^2)\cdot[b_2^{(1)}c_{\rm SW}/8+c_{2,4}^{(2)}{c_{\rm SW}}^2 + c_{2,7}^{(0)}+c_{2,14}^{(0)}+c_{2,14}^{(1)}c_{\rm SW}+c_{2,14}^{(2)}{c_{\rm SW}}^2] \quad (19)$$

[cf. Eq. (13)].

A potential complication is presented by gluon vertices. While the 3-gluon vertex dresses by a mere factor of $[1-w(g_0)]$, the dressed 4-gluon vertex contains a term which is not simply a multiple of its bare counterpart (see Appendix C of Ref. [11]). It is easy to check, however, that this term must simply be dropped, being precisely the one which has already been taken into account in dressing the 1-loop result; the remainder dresses in the same way as the 3-gluon vertex. The very same situation prevails with the dressed 5-point vertex of the clover action, as in diagram 4.

In conclusion, cactus resummation applied to the 2-loop quantity $\Sigma^{(2)}$ leads to the following rather simple recipe:

$$m_{c,\,\rm dressed}^{(2)}=\Sigma^{(1)}\frac{g_0^2}{1-w(g_0)}+(\Sigma^{(2)}-\Sigma_{\rm sub}^{(2)}) \times\frac{g_0^4}{[1-w(g_0)]^2}\Bigg|_{c_{\rm SW}\to c_{\rm SW}[1-w(g_0)]} . \quad (20)$$

[For the values of β in Table VI, $\beta=5.20,5.26,5.29,5.7,6.0,6.2,12.0,24.0$, we obtain from Eq. (18): $1-w(g_0)=0.697146$, 0.701957, 0.704298, 0.732579, 0.749775, 0.759969, 0.887765, 0.946087, respectively.]

Our results for $\kappa_{c,\,\rm dressed}^{(2)}$, as obtained from Eq. (20), are listed in Table VI. Comparing with the Monte Carlo estimates, dressed results show a definite improvement over non-dressed values. It is interesting to note that 1-loop dressed results already provide most of the improvement, except at very large β values. At the same time, a sizeable discrepancy still remains, as was expected from the start; multiplicative renormalizations, calculated to the same order, are expected to be much closer to their exact values. A first case study of this kind, regarding the β function with clover improvement, is now complete and will be presented elsewhere [6].

[1] B. Sheikholeslami and R. Wohlert, Nucl. Phys. **B259**, 572 (1985).
[2] E. Follana and H. Panagopoulos, Phys. Rev. D **63**, 017501 (2001).
[3] S. Caracciolo, A. Pelissetto, and A. Rago, Phys. Rev. D **64**, 094506 (2001).
[4] A. Bode, P. Weisz, and U. Wolff, Nucl. Phys. **B576**, 517 (2000).
[5] C. Christou, A. Feo, H. Panagopoulos, and E. Vicari, Nucl. Phys. **B525**, 387 (1998).
[6] A. Bode and H. Panagopoulos, ''The three-loop β-function of QCD with the clover action,'' hep-lat/0110211.
[7] M. Lüscher, S. Sint, R. Sommer, P. Weisz, and U. Wolff, Nucl. Phys. **B491**, 323 (1997).
[8] UKQCD Collaboration, K. C. Bowler *et al.*, Phys. Rev. D **62**, 054506 (2000).
[9] K. Jansen and R. Sommer, Nucl. Phys. **B530**, 185 (1998).
[10] UKQCD Collaboration, C. R. Allton *et al.*, hep-lat/0107021.
[11] H. Panagopoulos and E. Vicari, Phys. Rev. D **58**, 114501 (1998).
[12] H. Panagopoulos and E. Vicari, Phys. Rev. D **59**, 057503 (1999).
[13] H. Panagopoulos and E. Vicari, Nucl. Phys. B (Proc. Suppl.) **83**, 884 (2000).
[14] G. Parisi, in *High-Energy Physics—1980*, XX International Conference, Madison, 1980, edited by L. Durand and L. G. Pondrom (AIP, New York, 1981).
[15] G. P. Lepage and P. B. Mackenzie, Phys. Rev. D **48**, 2250 (1993).